Molecular Biology of the Cell
Vol. 8, 13–31, January 1997

Transport through the Yeast Endocytic Pathway Occurs through Morphologically Distinct Compartments and Requires an Active Secretory Pathway and Sec18p/*N*-Ethylmaleimide-sensitive Fusion Protein

Linda Hicke,* Bettina Zanolari, Marc Pypaert, Jack Rohrer, and Howard Riezman

Department of Biochemistry, Biozentrum, University of Basel, Basel, Switzerland

Submitted May 10, 1996; Accepted October 1, 1996
Monitoring Editor: Ari Helenius

Molecules travel through the yeast endocytic pathway from the cell surface to the lysosome-like vacuole by passing through two sequential intermediates. Immunofluorescent detection of an endocytosed pheromone receptor was used to morphologically identify these intermediates, the early and late endosomes. The early endosome is a peripheral organelle that is heterogeneous in appearance, whereas the late endosome is a large perivacuolar compartment that corresponds to the prevacuolar compartment previously shown to be an endocytic intermediate. We demonstrate that inhibiting transport through the early secretory pathway in *sec* mutants quickly impedes transport from the early endosome. Treatment of sensitive cells with brefeldin A also blocks transport from this compartment. We provide evidence that Sec18p/*N*-ethylmaleimide-sensitive fusion protein, a protein required for membrane fusion, is directly required in vivo for forward transport early in the endocytic pathway. Inhibiting protein synthesis does not affect transport from the early endosome but causes endocytosed proteins to accumulate in the late endosome. As newly synthesized proteins and the late steps of secretion are not required for early to late endosome transport, but endoplasmic reticulum through Golgi traffic is, we propose that efficient forward transport in the early endocytic pathway requires delivery of lipid from secretory organelles to endosomes.

INTRODUCTION

The endocytosis of extracellular molecules and plasma membrane proteins is required by cells to internalize nutrients, down-regulate receptors, and remove damaged proteins from the membrane. Primary endocytic vesicles that form at the plasma membrane transfer these components to an early endosome where some proteins are sorted for recycling back to the plasma membrane. Others continue through the endosomal pathway to the late endosome/prelysosome and then to the lysosome where they are degraded.

*Present address: Department of Biochemistry, Molecular Biology, and Cell Biology, Northwestern University, 2153 Sheridan Road, Evanston, IL 60208.

Membrane transport through the mammalian endocytic pathway has been studied in vivo and in vitro, and some of the proteins that function in endosomal transport have been identified (reviewed by Gruenberg and Maxfield, 1995). Many of these are proteins similar to those that mediate membrane transport in the secretory pathway. A number of small GTP-binding proteins are localized to the plasma membrane and endosomal compartments. Members of the Rab/Ypt family function in recycling to the plasma membrane and in lysosome-directed transport at the early and late endosomes (Simons and Zerial, 1993; Singer-Krüger *et al.*, 1994; Feng *et al.*, 1995). Members of the ARF family have been localized to early endocytic compartments and the plasma membrane (D'Souza-Schorey *et al.*, 1995; Peters *et al.*, 1995; Whitney *et al.*, 1995). Heterotrimeric G proteins have been suggested

© 1997 by The American Society for Cell Biology

to be required for the fusion of early endosomes in vitro (Colombo *et al.*, 1992). An ATPase, the *N*-ethylmaleimide-sensitive fusion protein (NSF) is also required in vitro for the fusion of early endosomes with each other (Diaz *et al.*, 1989; Rodriguez *et al.*, 1994) and another class of proteins with proposed fusogenic functions, the annexins, have also been implicated in endosomal transport (Gruenberg and Emans, 1993). Coatomer (COPI) proteins that mediate vesicle budding in the biosynthetic pathway have recently been found associated with endosomes and are required for the formation of endocytic carrier vesicles in vitro (Whitney *et al.*, 1995; Aniento *et al.*, 1996). Finally, phosphatidylinositide-3 (PI-3) kinases appear to regulate the transport of both secretory and endocytosed proteins destined for the lysosome (De Camilli *et al.*, 1996).

The association of proteins known to be required for vesicle budding and fusion in the secretory pathway with endocytic compartments suggests that some transport steps in the endocytic pathway are also mediated by vesicular transport. However, compared with the secretory pathway, inward transport via endosomes to the lysosome is not well characterized and controversy still exists about which transport steps are mediated by vesicles and which may occur through organelle maturation and fusion.

To provide more information about how endosomal transport occurs at the molecular level, we have studied the endocytic pathway of *Saccharomyces cerevisiae*. This yeast internalizes small molecules by both fluid phase and receptor-mediated endocytosis (Riezman, 1993). Proteins similar to those endocytosed in mammalian cells, including nutrient permeases, G-protein-coupled receptors, and peptide transporters, are internalized from the plasma membrane and transported to the vacuole where they are degraded. Endosomal transport in yeast can be studied by monitoring radioactively labeled α-factor pheromone that is bound and internalized by its G-protein-coupled receptor, Ste2p. Internalized α-factor-Ste2p complex does not recycle but is degraded in the vacuole. Degradation of internalized α-factor is inhibited by energy poisons that block membrane traffic and is severely retarded at 15°C, a temperature at which endocytic traffic in mammalian cells is also slowed. On its way from the plasma membrane to the vacuole, α-factor moves through two biochemically separable membrane-bounded compartments known as the yeast early and late endosomes (Singer and Riezman, 1990).

It has been previously shown that the endocytic and biosynthetic pathways to the vacuole overlap at the prevacuolar compartment, an organelle that accumulates vacuolar and endocytosed proteins in a subset of vacuolar protein sorting (*vps*) mutants (Piper *et al.*, 1995). This prevacuolar organelle may be one of the endocytic compartments that mediate the transport of α-factor. How proteins are transported between yeast endocytic compartments is not known, although several proteins that function in this process have been identified. These include the small GTP-binding proteins encoded by the *YPT7* and *VPS21/YPT51* genes (Wichmann *et al.*, 1992; Schimmöller and Riezman, 1993; Singer-Krüger *et al.*, 1994; Horazdovsky *et al.*, 1994), the PI-3 kinase Vps34p (Munn and Riezman, 1994), a dynamin homologue Dnm1p (Gammie *et al.*, 1995), and proteins encoded by the *VPS2/REN1* and *VPS4/END13* genes (Davis *et al.*, 1993; Munn and Riezman, 1994).

In this report we identify the yeast early and late endosomes morphologically, demonstrating that they are similar in character and distribution to mammalian endocytic organelles. We also demonstrate that the Sec18/NSF protein is required in vivo for an early postinternalization step leading to transport to the vacuole. Finally, we show that transport through the yeast early endosome requires an active secretory pathway, implying that endocytic traffic is tightly regulated by the delivery of some component from the early secretory organelles to the early endosome.

MATERIALS AND METHODS

Strains, Plasmids, Media, and Reagents

vps2 (Tom Stevens, University of Oregon, Eugene, OR), *erg6* (Rick Gaber, Northwestern University, Evanston, IL), and *sec* mutants (Randy Schekman, University of California, Berkeley, CA), except *sec18-20*, were crossed once or twice to RH448 to introduce *bar1-1* into the strains. *sec18-20* was isolated in a screen for mutants defective in the accumulation of a fluid-phase endocytic marker, lucifer yellow, in the vacuole (Chvatchko *et al.*, 1986). This mutant failed to secrete active invertase and did not complement *sec18-1* but was complemented by the *SEC18* gene carried on a plasmid. *sec18-20* does not grow at 30°C, like *sec18-1*, and transport of newly synthesized carboxypeptidase Y (CPY) out of the endoplasmic reticulum (ER) is blocked at 32°C with no preincubation at this temperature (our unpublished data). *pep4::URA3* derivatives of some *sec* strains were constructed by one-step gene disruption with pTS15 (Tom Stevens, University of Oregon). The genotypes of all strains are listed in Table 1.

YPUAD-rich medium, SD minimal medium, and SDYE medium have been described (Zanolari *et al.*, 1992; Hicke and Riezman, 1996).

EXPRE^{35}S^{35}S protein labeling mix was obtained from DuPont (Wilmington, DE). Recombinant lyticase was purified from *Escherichia coli* as described (Shen *et al.*, 1991) with the following modifications: Osmotic shock fluid was dialyzed overnight in 10 mM sodium acetate (pH 5) and loaded onto a Mono S HR55 column (Pharmacia LKB Biotechnology, Uppsala, Sweden) on a Pharmacia FPLC system equilibrated in the same buffer, and lyticase activity was eluted with a 0–200 mM NaCl gradient in the sodium acetate buffer. Lyticase activity was eluted at ≈40 mM NaCl.

^{35}S-labeled α-factor was purified as described (Singer and Riezman, 1990) and stored in a solution of 29.6% acetonitrile, 0.025% trifluoroacetic acid, 0.01% Triton X-100, and 10 ng/ml hemoglobin after freezing in liquid nitrogen. Reagents used in α-factor internalization and degradation assays and for the fractionation of endosomes by differential centrifugation and on Nycodenz gradients were obtained as described (Singer and Riezman, 1990).

Table 1. Yeast strains

Strain	Genotype[a]
RH448	*ura3, leu2, his4, lys2, bar1-1*
RH732	*pep4::URA3, ura3, leu2, his4, lys2, bar1-1*
RH1298	*ste2::LEU2, ura3, leu2, his4, bar1-1*
RH3209	*ura3::STE2-cmyc[URA3], ste2::LEU2, ura3, leu2, his4, bar1-1*
RH3089	*ura3::STE2-cmyc[URA3], ste2::LEU2, pep4-3, ura3, leu2, his4, lys2, bar1-1*
RH2401	*vps2, pep4, ura3, leu2, his4, bar1-1*
RH3387	*end4::HIS3, pep4, ura3, his3, suc2Δ, bar1-1*
RH3205	*end6-1, ura3::STE2-cymc[URA3], ura3, leu2, his4, lys2, bar1-1*
RH1491	*sec12-4, ura3, leu2, his4, lys2, bar1-1*
RH2044	*sec12-4, pep4::URA3, ura3, leu2, his4, lys2, bar1-1*
RH1737	*sec18-20, ura3, leu2, his4, bar1-1*
RH2043	*sec18-20, pep4::URA3, ura3, leu2, his4, bar1-1*
RH2465	*sec12-4, sec18-20, ura3, leu2, his, bar1-1*
RH1489	*sec13-1, ura3, leu2, his4, lys2, bar1-1*
RH1499	*sec16-2, ura3, leu2, his4, lys2, bar1-1*
RH1592	*sec17-1, ura3, leu2, his4, lys2, bar1-1*
RH1486	*sec20-1, ura3, leu2, his4, lys2, bar1-1*
RH1436	*sec23-1, ura3, leu2, his4, bar1-1*
RH1522	*sec7-1, ura3, leu2, his4, bar1-1*
RH1554	*sec4-2, ura3, his4, lys2, bar1-1*
RH1524	*sec5, ura3, leu2, his4, lys2, bar1-1*
RH1528	*sec9, urq3, leu2, his4, lys2, bar1-1*
RH3415	*ret1-1, ura3, leu2, his, bar1-1*
RH2688	*sec27, ura3, leu2, his4, bar1-1*
RH1885	*erg6, ura3, leu2, his4, bar1-1*

[a] All strains listed are *MAT***a**.

The c-myc epitope EQKLISEEDLN was introduced into the second extracellular loop of Ste2p between amino acids T^{199} and Q^{200} by PCR mutagenesis as described (Rohrer *et al.*, 1993). The sequence of the PCR-amplified part of the resulting plasmid was determined to ensure that the epitope had been introduced accurately with no additional mutations. The plasmid encoding the Ste2–c-myc protein was introduced into the *ura3* gene of strain RH1298 (*ste2Δ*) by single-step gene transplacement. The Ste2–c-myc protein complemented the *ste2Δ* defect in α-factor response exhibited by the parent strain (as measured by mating projection formation) and internalized α-factor with kinetics identical to wild-type Ste2p.

CPY and affinity-purified Ste2p antiserum have been described (Hicke and Riezman, 1996). Monoclonal antibody 9E10 that recognizes the c-myc epitope (Evan *et al.*, 1985) was generously provided by Sandoz Pharmaceutical (Basel, Switzerland) and Tommy Nilsson (European Molecular Biology Laboratory, Heidelberg, Germany). Anti-rabbit IgG conjugated to the fluorophore Cy3 (Jackson ImmunoResearch Labs, West Grove, PA) was used to visualize Ste2p during immunofluorescence experiments.

Immunofluorescence, Confocal, and Electron Microscopy

Cells were grown overnight at 24°C, centrifuged, and resuspended in YPUAD to 1×10^7 cells/ml. Cycloheximide was added to 20 μg/ml and the cells were incubated for 10 min at 15–30°C. For the experiment with *sec* strains shown in Figure 7, cells were then centrifuged and resuspended in 32°C YPUAD containing cycloheximide and incubation continued for 5 min at 32°C. Experiments with other strains did not include this step. An aliquot of cycloheximide-treated cells was withdrawn (10 ml) and the remaining cells were exposed to 1×10^{-7} M α-factor at 15–32°C. Aliquots of cells (10 ml) were removed at various times, and all samples were fixed by the addition of 0.1 vol of 37% formaldehyde/1 M potassium phosphate (pH 6.5) for 2 h at room temperature. Fixed cells were then washed three times with SP buffer (1.2 M sorbitol/0.1 M potassium phosphate, pH 6.5) and resuspended in 1.5 ml of SP containing 20 mM 2-mercaptoethanol and recombinant lyticase to remove the cell wall. After lyticase treatment for 1 h at 30°C, the cells were washed three times with SP and finally resuspended in 0.25 ml of SP. Fixed cells were incubated with Ste2p antiserum and Cy3-conjugated secondary antibody and prepared for immunofluorescence as described (Zanolari and Riezman, 1991).

For confocal microscopy cells were prepared as above except that *end6* cells were preincubated for 15 min at 37°C before the addition of cycloheximide, and incubation with cycloheximide, followed by the addition of α-factor, was continued at 37°C. Images of cells were obtained with a Noran scanning confocal microscope with illumination from a 568-nm wavelength source. Images from a series of focal planes (0.3 μm apart) of each cell were recorded. The photographs labeled slice are the image of a focal plane from the middle of the cell. The three-dimensional images (3D) are composites taken of all focal planes from the cell.

For immunoelectron microscopy, cells were prepared, fixed, and washed as described above, an aliquot was removed for immunofluorescence, and the remaining cells were treated with 0.5% glutaraldehyde in phosphate-buffered saline (PBS) for 24 h at 4°C. These cells were washed three times in PBS and embedded in 1% low-melting-temperature agarose. Small blocks (≈1 mm^3) were infused with 2.1 M sucrose in PBS overnight at 4°C and then frozen in liquid nitrogen on aluminum studs. Frozen sections (110-nm thick) were cut on a Reichert-Jung Ultracut microtome with a FC4E cryoattachment. They were labeled with a c-myc monoclonal antibody and anti-mouse IgG conjugated to 5- or 10-nm gold particles (Biocell Research Laboratories, Cardiff, United Kingdom) and then contrasted and embedded as described (Nilsson *et al.*, 1993). The sections were stained with lead citrate and examined in a Zeiss EM10 electron microscope.

Pulse-Biosynthesis Analysis of Carboxypeptidase Y

The transport of CPY through the biosynthetic pathway was monitored by pulse-chase analysis performed as described (Hicke and Riezman, 1996) with the following modification: Cells were preincubated for 5 min at 32°C before the addition of 50 μCi of EXPRE^{35}S^{35}S protein labeling mixture, and incubation at 32°C was continued during the following pulse-chase period.

α-Factor Internalization Assays

All assays were performed as described (Dulic *et al.*, 1991) on strains that were propagated overnight in YPUAD. Briefly, cells were grown at 24°C or 30°C to a density of $0.5–2 \times 10^7$ cells/ml. Cells were harvested, washed in YPUAD, and resuspended to 5×10^8 cells/ml in YPUAD prewarmed to 30°C or 32°C. Cells were then incubated for 5 min at 30°C or 32°C, $1–2 \times 10^5$ cpm of ^{35}S-labeled α-factor were added, and incubation was continued at 30–32°C for an additional 60 min. For the experiment performed with brefeldin A (BFA), α-factor was allowed to bind to cells on ice and unbound peptide was removed by centrifugation. Cells were resuspended in 0°C YPUAD, BFA from a 25 mg/ml stock in methanol, or methanol alone, was added, incubation on ice was continued for 4 to 5 min, and cells were shifted to 30°C to initiate internalization. Aliquots of cells were withdrawn after different times, washed in pH 1 buffer to remove surface-bound α-factor or in pH 6 buffer and filtered, and the amount of cell-associated radioactivity was determined by scintillation counting. A time course of internalization was generated for each strain by expressing the amount of internalized α-factor as a ratio of cpm detected in pH 1-washed cells to that detected in pH 6-washed cells for each time point.

α-Factor Degradation Assays

Cells were grown overnight at 24°C or 30°C in YPUAD to a density of 0.3–2 × 10^7 cells/ml, harvested, washed once in YPUAD at room temperature, and resuspended to 0.5–1 × 10^9 cells/ml in YPUAD prewarmed to 30–37°C. Cells were incubated at 30–37°C for the amount of time indicated in the figure legend and ^{35}S-labeled α-factor (≈10^6 cpm) was added to each strain. Incubation at the designated temperature was continued for 5 min to allow α-factor binding. Cells were then centrifuged for 4 min at 30–37°C in a tabletop centrifuge and immediately resuspended at 0.5–1 × 10^9 cells/ml in prewarmed YPUAD. Incubation with shaking was continued at 30–37°C and 100-ml aliquots were withdrawn after various times of chase. Cell aliquots were diluted into 10 ml of 50 mM sodium citrate (pH 1) and filtered, and internalized α-factor was extracted and analyzed by thin layer chromatography (TLC) as described previously (Dulic *et al.*, 1991). For the assays performed in the presence of BFA, cells were allowed to bind α-factor and then were resuspended and incubated with BFA as described for the α-factor internalization assays.

Fractionation of Endosomes by Differential Centrifugation and Flotation on Nycodenz Gradients

Cells were grown overnight at 24°C or 30°C in YPUAD to a density of 0.5–2 × 10^7 cells/ml. Cells (2–4 × 10^{10}) were harvested and washed once in YPUAD. To analyze the effect of cycloheximide on endocytic transport, cells were resuspended in 30°C YPUAD, 10 μg/ml cycloheximide were added to one sample, and cells were incubated for 5 min at 30°C. ^{35}S-labeled α-factor was added (2–5 × 10^6 cpm) and allowed to bind to cells for 5 min at 30°C. Unbound α-factor was removed by centrifugation at 30°C. Cells were then resuspended in 30 ml of YPUAD with or without cycloheximide and incubated with shaking at 30°C. After 0, 20, and 60 min, aliquots (10 ml) were removed and diluted into 90 ml of ice-cold sorbitol medium [0.8 M sorbitol/5 mM 2-amino-2-methyl-1,3-propanediol-piperazine-*N*,*N*′-bis(ethanesulfonic acid) buffered to pH 6.8 with PIPES] containing 10 mM NaN_3 and 10 mM NaF. Cells from each time point were then converted to spheroplasts and lysed, and the resulting lysates were subjected to differential centrifugation as previously described (Singer and Riezman, 1990) with the following modification: To increase the recovery of endosomes in the 100,000 × *g* pellet (P3) fraction, spheroplasts were lysed in sorbitol medium by homogenization (six strokes, five to seven times) in a Wheaton tissue grinder fitted with an A pestle (Wheaton, Millville, NJ). The P3 fraction was resuspended in 1.6 ml of 37% (wt/vol) Nycodenz with four to six strokes in a Potter-Elvehjem homogenizer. The membranes in the resuspended pellet were then overlaid with Nycodenz solutions of decreasing density and centrifuged, and gradient fractions were collected as described (Singer and Riezman, 1990). The 100,000 × *g* supernatant (S3) resulting from this treatment was centrifuged overnight (15–16 h) at 150,000 × *g* in a TLA100 rotor fitted with microcentrifuge tube adapters (Beckman Instruments, Palo Alto, CA) to generate P4 pellet and S4 supernatant fractions.

To analyze endosomal transport in *sec18* and wild-type strains, cells were harvested and washed as described above and then resuspended in 40 ml of YPUAD precooled on ice. ^{35}S-labeled α-factor was added and allowed to bind to cells for 45 min to 1 h on ice with gentle rocking. Unbound α-factor was removed by centrifugation at 3°C for 4 min at 4000 × *g* in a GSA rotor (Beckman Instruments). Cells were resuspended in 40 ml of YPUAD prewarmed to 32°C and incubated with shaking at 32°C. After 5, 15, 30, and 60 min, aliquots were removed. Lysates were prepared from each aliquot and subjected to differential centrifugation and Nycodenz gradient fractionation as described above.

To follow the transport of α-factor in *sec12* and wild-type cells that had been preincubated at 32°C before internalization, cells were grown, harvested, and washed as described above. Cells were then resuspended in 40 ml of YPUAD prewarmed to 32°C, incubated for 5 min at 32°C, and ^{35}S-labeled α-factor was added. Incubation with α-factor was continued for 5 min at 32°C to allow binding, and unbound peptide was removed by centrifugation at 32–34°C. The cell pellet was resuspended in 40 ml of 32°C YPUAD and incubation with shaking was continued at 32°C. Aliquots of cells (10 ml) were removed at 0, 15, 30, and 60 min of chase, converted to spheroplasts, and lysed. Differential centrifugation of the lysates and fractionation of P3 fractions on Nycodenz gradients was carried out as described above.

To test the effect of BFA on endosomal transport, an experiment similar to the previous one was performed on *erg6* cells propagated at 30°C. After harvesting and washing, however, cells were resuspended in 30°C medium to which methanol or BFA in methanol (75 μg/ml, final concentration) had been added. Cells were then incubated for 5 min at 30°C; α-factor was added, allowed to bind for 5 min at the same temperature, and removed by centrifugation as described above. Cells were then resuspended in 30°C medium containing either BFA or methanol alone, and aliquots were removed after 10 and 60 min.

In each fractionation experiment, the extent of cell lysis was determined by analyzing the percent of the cytosolic protein hexokinase that was released into the S1 supernatant. The amount of radioactivity found in pellet and supernatant fractions was expressed as a percent of the total radioactivity in the lysate after correction for cell lysis as described previously (Singer and Riezman, 1990). The profiles of radioactivity resulting from Nycodenz gradient fractionation were also normalized for the amount of cell lysis in each time point sample.

RESULTS

Transport of the α-Factor Receptor through the Endocytic Pathway

Two sequential membrane-bounded intermediates in the transport pathway from plasma membrane to vacuole have been identified by the fractionation of cell membranes (Singer and Riezman, 1990; Singer-Krüger *et al.*, 1993). These compartments have been designated the yeast early and late endosomes. To identify the yeast endosomes morphologically, we followed transport of the α-factor receptor through the pathway by performing immunofluorescence with anti-receptor antiserum. Cells were incubated with cycloheximide to inhibit new receptor synthesis and then exposed to α-factor to stimulate internalization of cell-surface Ste2p. Figure 1a shows that before the addition of α-factor to cells the receptor was found in an uneven distribution on the cell surface. In some cases it was also observed in small dot-like structures that appeared to be intracellular. This may be receptor that had been internalized constitutively and was en route through the endocytic pathway. Upon binding α-factor, all receptor was internalized and was observed at later time points in large structures that resided immediately adjacent to the vacuole. Staining of these compartments faded eventually (compare 16 and 30 min in the 30°C experiment), probably due to vacuolar degradation of the receptor. Staining of smaller more peripheral structures was seen at very early times after α-factor addition (4 min). As these small structures

may be early compartments of the endocytic pathway, we attempted to visualize them more extensively by performing immunofluorescence on cells incubated at 15°C, a temperature that retards transport through endosomes. At 16 min after exposure of cells to pheromone at this temperature, the ring-like staining at the cell surface had disappeared and extensive staining was seen in a large number of small peripheral structures, as well as a larger perivacuolar dot. After longer times, the staining disappeared from the smaller organelles and concentrated in the large structure that resided next to the vacuole. These results are consistent with the idea that the receptor moves through small peripheral early organelles and then into a large perivacuolar late organelle before it enters the vacuole.

Receptor was not observed in the vacuole itself because it was rapidly degraded once it reached this organelle. To demonstrate visually that the final destination of Ste2p was the vacuole, we identified receptor by immunofluorescence in *pep4* mutant cells that lack active vacuolar hydrolases. As the receptor undergoes slow constitutive endocytosis, we expected to find undegraded receptor in the vacuole and on the cell surface in the absence of α-factor. Figure 1b demonstrates that this was the case. Upon treatment of *pep4* cells with pheromone, the receptor disappeared from the cell surface and staining was seen only in the vacuole. To show that receptor that accumulated in the vacuole in *pep4* cells arrived there through the endocytic pathway, and not through an aberrant biosynthetic pathway, a *pep4end4*Δ mutant was constructed. The *end4*Δ mutant is unable to internalize pheromone at any temperature and receptor remains at the cell surface even after α-factor binding (our unpublished data). In the *pep4end4* double mutant, the receptor was visualized primarily at the cell surface both before and after the exposure of cells to pheromone, demonstrating that the accumulation of receptor in the vacuole in *pep4* mutants required its internalization from the plasma membrane.

The perivacuolar structure in which receptor was observed after α-factor binding and internalization is strikingly similar to the prevacuolar compartment in which newly synthesized vacuolar proteins accumulate in a subset of mutants that are defective in vacuolar protein sorting (*vps* mutants) (Raymond *et al.*, 1992). This compartment is a functional organelle through which both vacuolar proteins and endocytosed **a**-factor receptor (Ste3p) pass en route to the vacuole (Piper *et al.*, 1995). To determine whether endocytosed α-factor receptor is transported through the prevacuolar compartment, we looked at receptor distribution in the *vps27pep4* and *vps2pep4* mutants that accumulate vacuolar proteins in this structure. The results obtained from both mutants were identical and the data for the *vps2pep4* mutant are shown in Figure 1b. Before exposing the cells to α-factor, receptor was found on both the cell surface and in the prevacuolar compartment. After the addition of pheromone, receptor disappeared from the cell surface and was seen in one large perivacuolar dot, consistent with the idea that the surface receptor had been transported to the prevacuolar compartment. Although we have not performed double labeling of Ste2p and a vacuolar protein to determine that they colocalize in the same structure in *vps* cells, this result is in agreement with the previous observation that the prevacuolar compartment corresponds to a late endocytic intermediate that is a point at which both endocytic and biosynthetic pathways intersect (Piper *et al.*, 1995).

Confocal microscopy was used to confirm that the small peripheral and large perivacuolar staining of receptor observed after α-factor addition corresponded to intracellular organelles. Immunofluorescence of wild-type cells was performed as for Figure 1 and the cells were visualized by using a confocal microscope. Figure 2a shows the staining of receptor in a 3D reconstruction and in a single slice or section through the same cell, both before and at various times after treatment of cells with α-factor. Before α-factor treatment, Ste2p was seen in small patches on the cell surface. Surface localization was confirmed by the ring of staining observed in the slice. Eight minutes after α-factor addition, receptor had moved into small intracellular compartments and a more brightly stained perivacuolar organelle. After 16 minutes, receptor had moved almost completely into the perivacuolar organelle. The slice pictures show that these compartments reside within the cell. Like *end4*, the *end6* temperature-sensitive mutant is also unable to internalize α-factor at the nonpermissive temperature (Munn *et al.*, 1995). Confocal microscopy of *end6* cells shows that, at the nonpermissive temperature, receptor was found to have a surface staining pattern exclusively, even at 16 min after exposure to α-factor.

The morphology of the large perivacuolar organelle was investigated in more detail by immunoelectron microscopy. Figure 2b shows electron micrographs of wild-type cells after 16 min of exposure to α-factor. In many cell profiles, electron-dense multivesicular membrane-bounded organelles were found next to the vacuole. Their appearance was similar to that of mammalian late endosome/prelysosome (Helenius *et al.*, 1983). Gold labeling was concentrated over these structures, indicating the presence of Ste2p. They were usually organized into large clusters that were similar in size to that of the bright perivacuolar bodies seen by immunofluorescence microscopy (0.5–1 mm). This, along with the similarity in intracellular location, indicates that these electron-dense organelles probably correspond to the perivacuolar organelles observed by light microscopy.

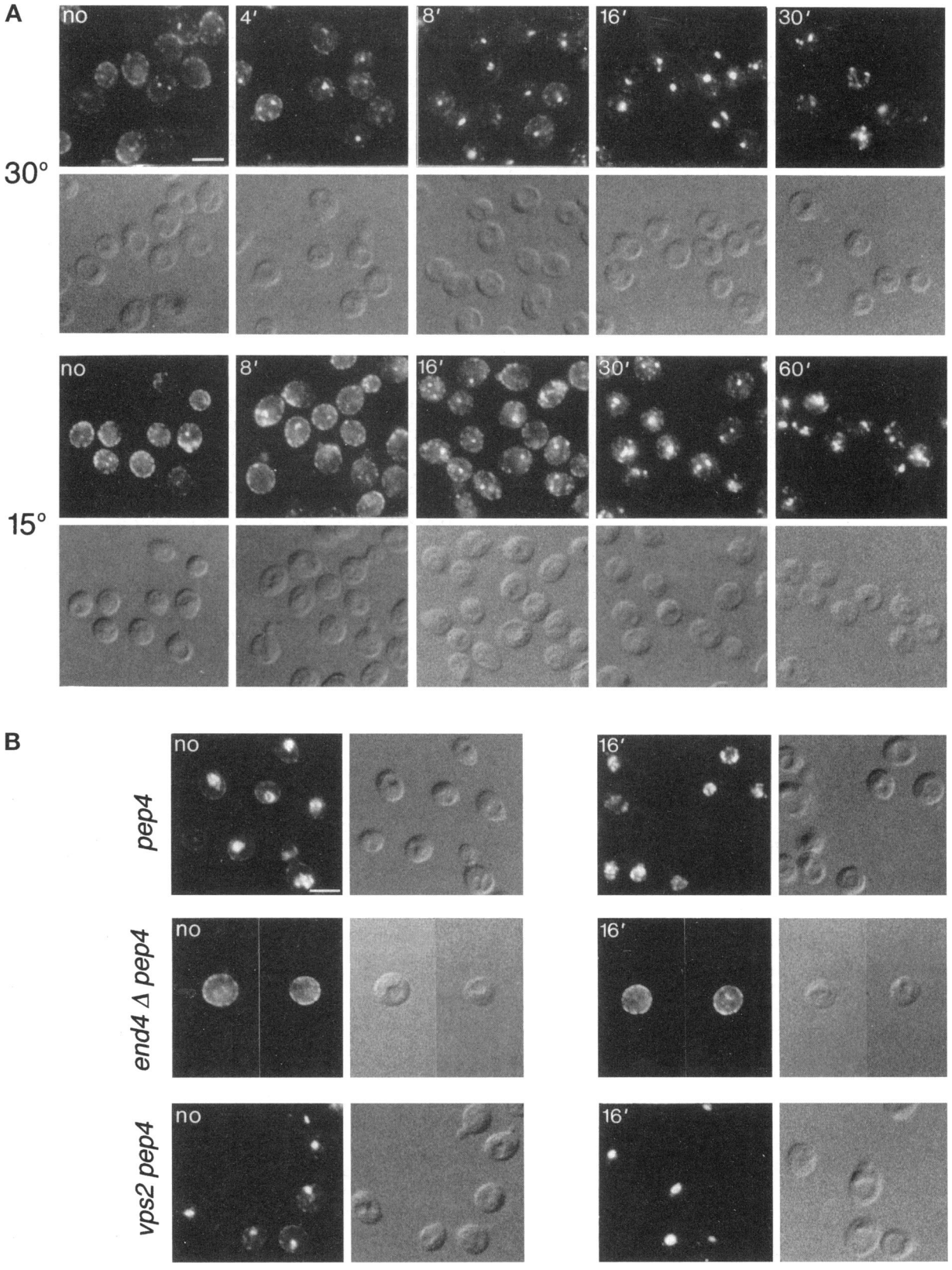
A
30°
no
4′
8′
16′
30′
15°
no
8′
16′
30′
60′
B
pep4
no
16′
end4 Δ pep4
no
16′
vps2 pep4
no
16′

Figure 1.

To correlate the perivacuolar endocytic organelle with the early and late endocytic intermediates that have been identified by subcellular fractionation, we analyzed the transport of α-factor peptide under conditions similar to those used to detect its receptor by immunofluorescence. α-Factor is normally transported rapidly through an early and a late endosome to the vacuole where it is degraded. Transport of radiolabeled peptide through each endosome can be followed by the separation of endosomes by differential centrifugation and subsequent fractionation on Nycodenz gradients (Singer and Riezman, 1990). The experiments, depicted in Figures 1 and 2, that followed the transport of internalized α-factor receptors were performed on cells pretreated with cycloheximide to inhibit new receptor synthesis. We therefore examined the effect of cycloheximide on the transport of the internalized ligand radiolabeled α-factor. Cycloheximide at concentrations up to 100 μg/ml had no effect on the ability of cells to internalize α-factor (our unpublished data); however, surprisingly, the drug inhibited the rate of degradation of internalized peptide (Figure 3a). After a 5-min preincubation with 100 μg/ml cycloheximide, α-factor degradation was obviously retarded and longer preincubation (15 min) exacerbated the effect. The same effect was observed in cells treated with 10 μg/ml cycloheximide. As internalized ligand is degraded in the vacuole, this delay in degradation implied that transport of peptide between the plasma membrane and the vacuole was slower than in the absence of cycloheximide. Differential centrifugation of lysates prepared from cells that internalized α-factor in the presence or absence of cycloheximide showed that α-factor did accumulate in endosomes in the presence of the drug (Figure 3b). During this type of experiment, vacuoles sediment rapidly and are collected after centrifugation at 7500 × *g* (P1 fraction), whereas endosomes are found in the pellet (P3 fraction) of a 100,000 × *g* centrifugation (Singer and Riezman, 1990). In untreated cells, radiolabeled α-factor initially was found mostly in the P3 fraction. Sixty minutes after internalization, the radioactive ligand was recovered primarily in the P1 fraction. In contrast in the presence of cycloheximide, α-factor remained associated with the P3 fraction for much longer and was still found primarily in this pellet even after a 60-min internalization.

Early and late endosomes that have been collected in P3 can be separated from each other by fractionation on Nycodenz gradients. In the absence of cycloheximide, α-factor was found in both endosomal populations at early time points after internalization and was quickly transported out of both organelles. In cells treated with the drug, α-factor was also detected in both compartments at early time points but then accumulated in the late endosome fractions (Figure 3c). Cycloheximide may delay transport from the late endosome to the vacuole. Alternatively, α-factor may normally disappear from the late endosome not only because of transport but also because of degradation by newly synthesized proteases that mix with the peptide in this organelle. Inhibiting the synthesis of new vacuolar proteins would then inhibit the degradation of α-factor in the late endosome. Regardless of the cause, almost all internalized α-factor was found in the late endosome 20 min after internalization. At 16 min after pheromone addition, immunofluorescence experiments showed that α-factor receptor accumulated in the large perivacuolar structure (Figures 1a and 2a). Therefore, we suggest that this structure represents the yeast late endosome.

Because cycloheximide adversely affects transport of α-factor through the endocytic pathway, it is possible that Ste2p accumulates in an aberrant nonfunctional structure induced by cycloheximide and that this structure has physical characteristics similar to the late endosome. To determine whether internalized receptor is detected in a large prevacuolar structure even in the absence of cycloheximide, we performed immunofluorescence with anti-receptor antiserum on cells stimulated with α-factor in the absence of drug treatment (Figure 4). In the absence of cycloheximide, the receptor travels through structures similar in appearance to those observed in the presence of the drug. The large perivacuolar structure is clearly observed in these cells though not as prominently as in cells treated with cycloheximide. This is consistent with the observation that transport through this compartment is more rapid in the absence of cycloheximide. Because α-factor induces the expression of Ste2p, newly synthesized protein is observed in perinuclear structures that probably correspond to ER at later times after α-factor addition (e.g., at 16 min).

Figure 1 (cont). Immunofluorescence localization of α-factor receptor during its transport through the endocytic pathway. The transport of α-factor receptor was visualized in cells after stimulating internalization by exposing cells to α-factor pheromone. At the times after addition of α-factor indicated, cells were fixed and Ste2p was detected by using affinity-purified Ste2p antiserum. For each time point both fluorescent and Nomarski images are shown. Vacuoles are the organelles observed as indentations in the Nomarski image of the cell. Bars, 5 μm. (A) Immunofluorescence microscopy of Ste2p internalized in wild-type cells (RH448) at 30°C and at 15°C. At 15°C, membrane transport through endosomes is retarded. The first photograph shown in each series represents the pattern of Ste2p staining observed in cells before the addition of α-factor (no). (B) Immunofluorescence microscopy of Ste2p expressed in *pep4* (RH3089), *end4pep4* (RH3387), and *vps2pep4* (RH2401) cells. The pattern of Ste2p localization in each strain is shown both before exposure of cells to α-factor (no) and at 16 min after α-factor addition at 30°C. Notice that the receptor detected in the *vps2pep4* mutant is in a compartment that lies immediately adjacent to the vacuole, not in the vacuole itself.

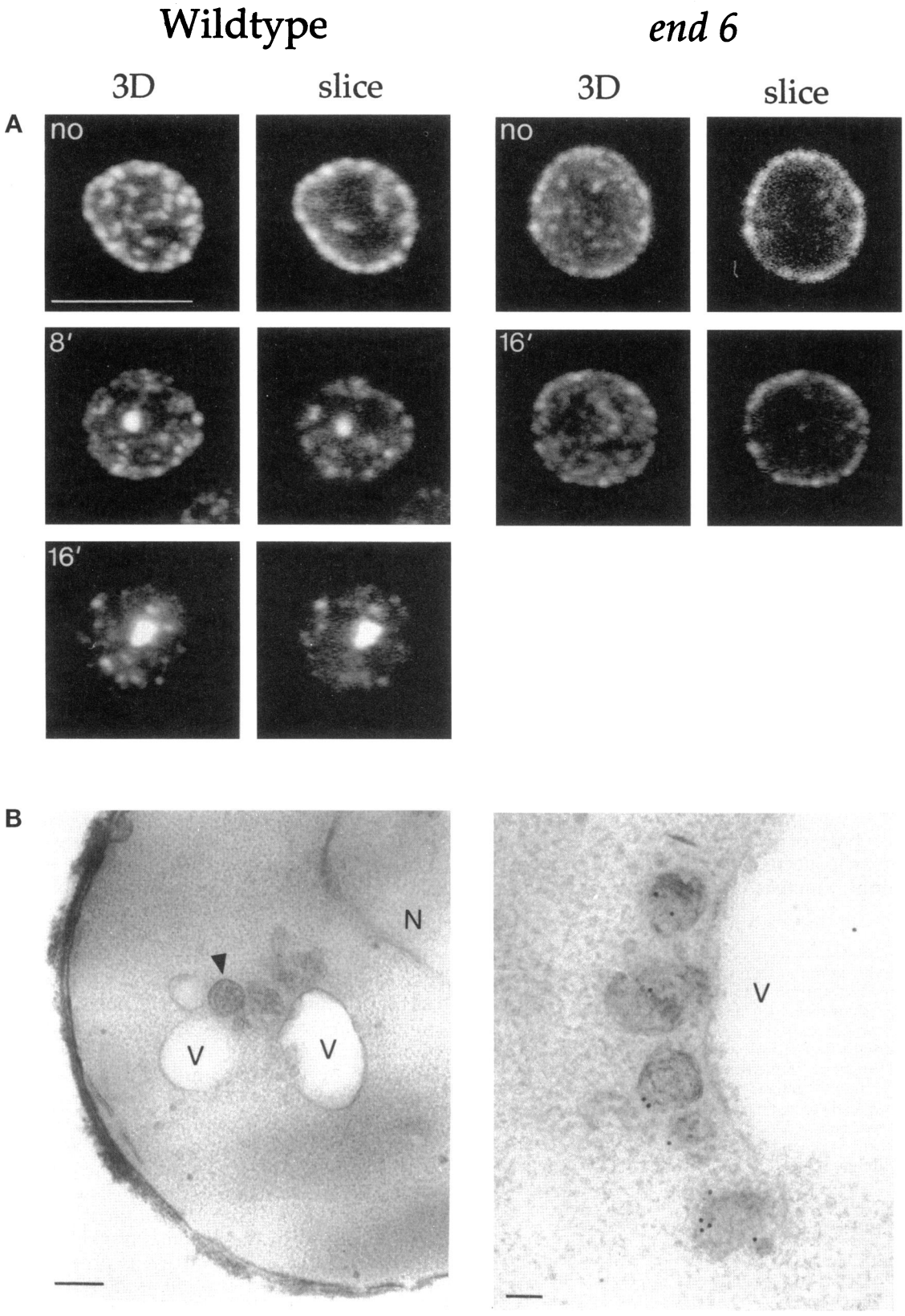

Figure 2.

An Active Early Secretory Pathway Is Required to Promote Membrane Traffic through the Endocytic Pathway

To determine whether Sec proteins that function to mediate vesicle budding and fusion during transport through the biosynthetic pathway are required in the endocytic pathway, we analyzed the ability of *sec* mutants to internalize radiolabeled α-factor and transport it to the vacuole. We focused our attention on mutants that block ER → Golgi transport because these mutations inhibit the first step of the secretory pathway that requires membrane transport and, therefore, potentially may affect multiple membrane transport events. Preliminary experiments indicated that none of the Sec proteins that are required for ER → Golgi transport, specifically *sec12*, *sec13*, *sec16*, *sec17*, *sec18*, *sec20*, *sec21*, *sec22*, *sec23*, *ypt1*, and *sar1*, are required for α-factor internalization (our unpublished data). Although at 37°C several of the *sec* mutants internalized α-factor more slowly and to a lesser extent than wild-type cells at the nonpermissive temperature, none of these mutants exhibited a severe defect such as that seen in endocytosis mutants (Raths *et al.*, 1993; Munn and Riezman, 1994; Munn *et al.*, 1995). In contrast, all of the ER → Golgi *sec* mutants showed a strong reduction in the rate of α-factor degradation at 37°C (Table 2). To extend this observation, we chose to analyze only the most restrictive *sec* mutants. *sec12* and *sec18* cells do not grow at 32°C. To determine how severely the secretory pathway is inhibited at this temperature, we analyzed transport of the vacuolar protein CPY. Figure 5a shows a pulse-chase analysis of CPY performed on wild-type, *sec12*, and *sec18* cells after a 5-min preincubation at 32°C. In wild-type cells, the core-glycosylated ER form of CPY (p1) observed after a 5-min pulse and 0-min chase had been almost completely converted to the mature vacuolar form after a 15-min chase. A small amount of the Golgi p2 form remained. In *sec12* and *sec18* cells, however, CPY remained exclusively in the ER form after a 15-min chase demonstrating a complete block in transport under these conditions. Figure 5b shows that α-factor internalization under the same conditions was similar in wild-type and *sec12* cells and somewhat slower in *sec18* cells. Degradation of internalized α-factor, however, was strongly inhibited in both *sec12* and *sec18* cells at 32°C (Figure 5c). In this experiment, α-factor degradation products were difficult to detect even in wild-type cells (for another example, see Figure 5). In Figure 5c, degradation products are barely detectable in *sec12* cells. They were, however, more pronounced in other experiments indicating that a small amount of degradation did occur in the *sec12* mutant.

The observation that all of the ER → Golgi Sec proteins were required for efficient α-factor degradation, including Sec12p, which is thought to reside exclusively in organelles of the early secretory pathway (Nakano *et al.*, 1988; Nishikawa and Nakano, 1993), suggested that ongoing membrane transport through the secretory pathway might be essential for efficient endocytic transport. To determine whether proteins that function at later stages of the secretory pathway are also necessary for endocytic transport, we tested the ability of *sec* mutants that block intraGolgi and Golgi → plasma membrane transport to degrade α-factor. The *sec7* mutation blocks intraGolgi transport and *sec4* inhibits the fusion of Golgi-derived secretory vesicles with the plasma membrane. Assays that measured the transport of CPY or the secretion of the periplasmic protein invertase showed that each of these mutant proteins was completely inactivated after a 15-min preshift at 37°C (our unpublished data). Figure 6 shows the ability of wild-type, *sec7*, and *sec4* cells to degrade α-factor under these conditions. Like *sec12*, the *sec7* mutant was strongly affected in its ability to degrade internalized α-factor. The *sec4* mutant, however, degraded α-factor nearly as rapidly as wild-type cells. Other *sec* mutants, *sec5* and *sec9*, that block Golgi → plasma membrane transport also degraded internalized α-factor normally (Table 2). These data show that the function of Sec proteins involved in ER → Golgi and intraGolgi transport are required for endocytic membrane transport. In contrast, the functions of the Sec4p, Sec5p, and Sec9p proteins that are required for Golgi → plasma membrane transport are not necessary for endocytic traffic.

Figure 2 (cont). Confocal and immunoelectron microscopy of wild-type and *end6* cells showing cell surface and internalized α-factor receptor. (A) Confocal immunofluorescence microscopy of Ste2p localized in wild-type cells (RH3209) incubated at 30°C and in temperature-sensitive *end6* cells (RH3205) incubated at 37°C. The localization of receptor before exposure to α-factor is shown in the photographs labeled no and after the addition of α-factor at the indicated times. 3D designates a 3D reconstruction composed of images from different focal planes of each cell, and slice indicates a two-dimensional image taken through the center of the same cell. Bar, 5 μm. (B) Internalized Ste2p visualized by immunoelectron microscopy in wild-type cells (RH3209) carrying a c-myc-tagged receptor at 16 min after exposure to α-factor. The low-magnification micrograph (39,000×; bar, 250 nm) shows a cluster of perivacuolar vesicles, one of which shows a distinct multivesicular appearance (arrowhead). The high-magnification micrograph (80,000×; bar, 80 nm) indicates that the perivacuolar vesicles label with Ste2p-antibody-conjugated gold. N, nucleus; V, vacuole.

Sec18p/NSF and the Early Secretory Pathway Are Required for Transport through the Early Endosome

To test which stage of the endocytic pathway is inhibited in the *sec12* and *sec18* mutants, we isolated endosomes from mutant cells that had internalized α-factor at the nonpermissive temperature. Figure 7a shows the transport of α-factor through endosomes in wild-type and *sec12* cells that had been preincubated at 32°C before the addition of pheromone. α-Factor was

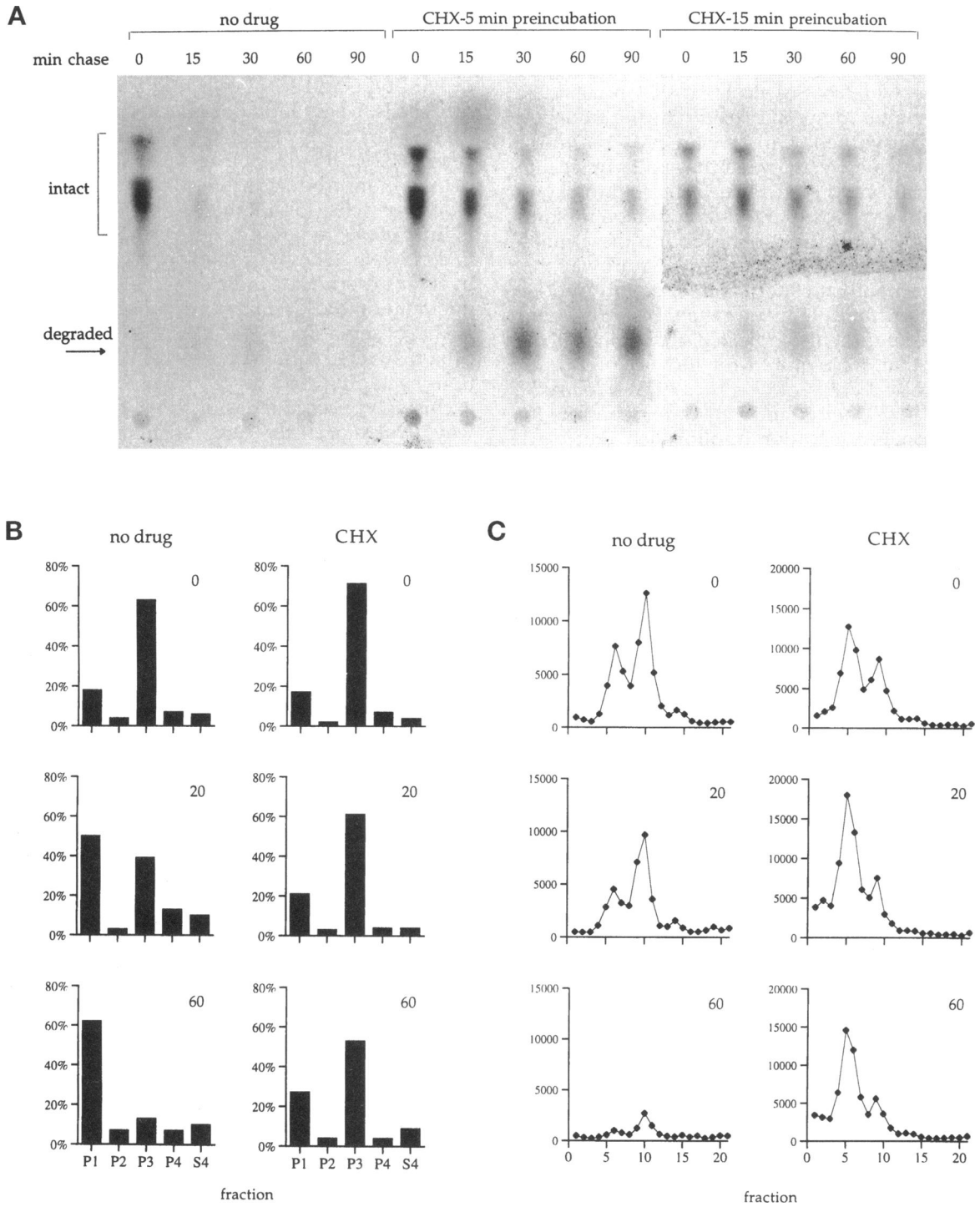

Figure 3. Inhibition of protein synthesis retards the degradation of internalized pheromone and causes accumulation of α-factor in the late endosome. (A) Wild-type cells (RH448) were preincubated at 30°C for 5 or 15 min with no drug or with 100 μg/ml cycloheximide (CHX). Radiolabeled α-factor was added and allowed to bind for 5 min, unbound pheromone was removed by centrifugation, and cells were resuspended in YPUAD with or without cycloheximide. Cell aliquots were removed at various times, and internalized α-factor was extracted from cell lysates and analyzed by TLC. The 0-min time point corresponded to ≈10 min of internalization at which time 70–80% of the bound pheromone had been internalized. The position at which undegraded α-factor migrates is indicated by the bracket and a degradation product is indicated by the arrow. (B) Cells preincubated 5 min with or without 10 μg/ml cycloheximide were treated as described above except at 0, 20, and 60 min after resuspending cells, aliquots were removed, cell lysates were prepared, and the lysates were subjected to differential

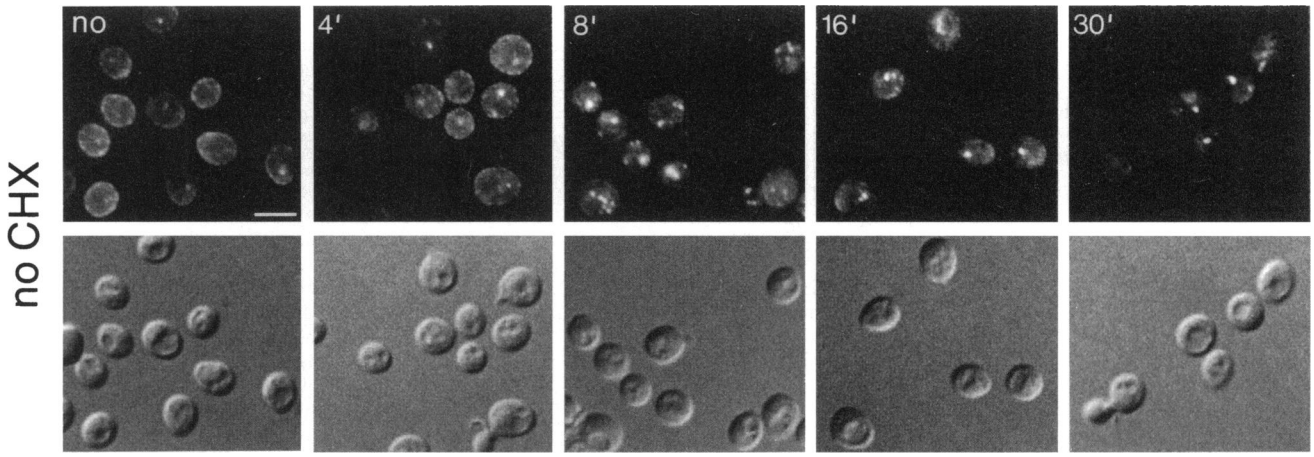

Figure 4. α-Factor receptor is transported through the large perivacuolar compartment in the absence of cycloheximide (CHX). Wild-type cells (RH448) were exposed to α-factor for various times, cells were fixed, and Ste2p was visualized by incubation with anti-Ste2p antiserum. Both immunofluorescence and Nomarski images are shown for each time point. Ste2p expression is induced after exposure of cells to α-factor; therefore, newly synthesized receptor can be detected in perinuclear structures that are probably the ER 16 and 30 min after α-factor treatment.

allowed to bind to the cells at 32°C, unbound peptide was removed, and bound peptide was chased through the endocytic pathway at the same temperature. In wild-type cells, α-factor was found in both early and late endosomes at early times after internalization and was chased rapidly from both endosomes. In *sec12* cells, α-factor was found primarily in the early endosome at early time points and remained there for more than 1 h after internalization.

A similar experiment was performed with *sec18* cells; however, the preincubation step was eliminated because mutant Sec18 protein is inactivated very rapidly at 32°C. Wild-type and *sec18* cells were allowed to bind radiolabeled α-factor on ice, unbound ligand was removed by centrifugation, and the cells were resuspended in 32°C medium to initiate the chase through the endocytic pathway. At the first time point (5 min), α-factor was found in about equal amounts in both early and late endosomes in wild-type cells. It was transported through both of these compartments by 30 min. In *sec18* cells, radiolabeled peptide was found only in the early endosome at 5 min, no peptide was detected in the late endosomal fractions, and it remained in the early compartment after a 60-min chase at 32°C (Figure 7b). In addition, internalized α-factor in *sec18* accumulated in a novel dense compartment (peak in fraction 12) at the later periods of chase. α-Factor found in this peak may be in an aberrant membrane generated only in mutant cells. Alterna-

(Figure 3 cont.) centrifugation. The amount of radioactivity associated with each pellet fraction and the final supernatant fraction was measured and is depicted as a percentage of the radioactivity measured in the original lysate. The P1 fraction contained the vacuoles and most of the plasma membrane and the P3 fraction contained endosomes. (C) The P3 membrane pellet represented for each time point in B was loaded onto Nycodenz gradients to separate the early and late endosomal fractions. The *y* axis represents the cpm associated with each fraction. The early endosomes are found in fractions 8–11 and the late endosomes are in fractions 4–7. The 0-min chase time point corresponds to ≈10 min after the initiation of pheromone internalization (see MATERIALS AND METHODS).

Table 2. Degradation of internalized α-factor in *sec* mutant strains

Strain temperature	Step of secretory pathway affected	α-Factor degradation at nonpermissive
Wild type	None	+
sec12	ER → Golgi	d
sec13	ER → Golgi	d
sec16	ER → Golgi	d
sec17	ER → Golgi	d
sec18	ER → Golgi	−
sec20	ER → Golgi	d
sec23	ER → Golgi	d
sec7	intraGolgi	d
sec14	intraGolgi	d
sec4	Golgi → plasma membrane	+
sec5	Golgi → plasma membrane	+
sec9	Golgi → plasma membrane	+
sec27	ER retention	+
ret1	ER retention	+
erg6/no drug	None	+
erg6 + BFA	ER → Golgi	−

Degradation is indicated as follows: +, degradation similar to wild type; d, degradation strongly defective but detectable; −, no detectable degradation. Degradation assays were performed on each strain at 30–37°C with a 0 to 15-min preshift at the nonpermissive condition.

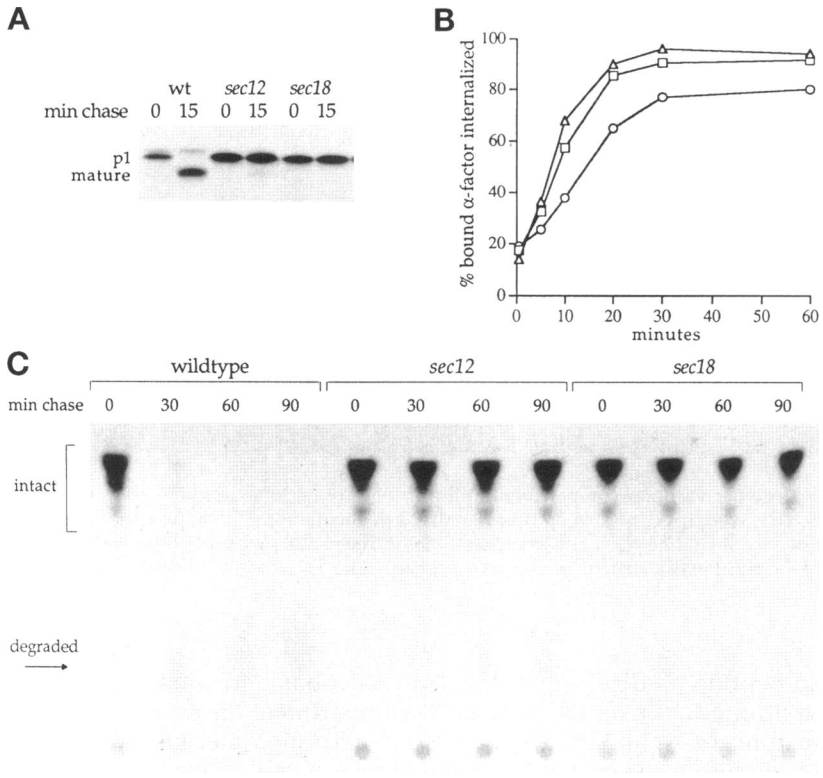

Figure 5. *sec* mutants that block ER → Golgi transport are defective in the degradation but not internalization of endocytosed α-factor. (A) Pulse-chase analysis of CPY in wild-type (RH448), *sec12* (RH1491), and *sec18* (RH1737) cells. Cells were preincubated at 32°C for 5 min, ^{35}S protein labeling mixture was added for 5 min, and then a chase was initiated. Newly synthesized CPY present in cells after a 0- or 15-min chase is shown. p1 CPY is the ER core-glycosylated form of the protein, and mature CPY is that which has reached the vacuole and been cleaved to remove the propeptide. (B) α-Factor internalization assays performed on wild-type (triangles), *sec12* (squares), and *sec18* (circles) cells preincubated 5 min at 32°C. The vertical axis represents the percentage of bound pheromone internalized at each time point. Each data point represents the average of two independent assays. (C) α-Factor degradation assays performed on wild-type, *sec12*, and *sec18* cells preincubated 15 min at 32°C. After α-factor binding, cells were resuspended in 32°C medium and cell lysates were prepared from aliquots taken at the indicated times. Internalized α-factor extracted from the lysates was subjected to TLC to separate the intact (bracket) and degraded (arrow) forms of the peptide. The 0-min time point corresponded to ≈10 min of internalization at which time ≈60% of the bound pheromone had been internalized in wild-type and *sec12* cells and ≈40% of the bound pheromone had been internalized in *sec18* cells.

tively, the α-factor found in this peak may reside in an early, as yet uncharacterized, endocytic intermediate that was not easily detectable in wild-type cells.

These data demonstrate that blocking ER → Golgi transport in *sec12* and *sec18* mutants rapidly induces a severe retardation of membrane traffic through the early endosome. As mentioned above, it is unlikely that the Sec12 protein functions directly in the endocytic pathway. Sec18p, however, is a cytosolic/peripheral membrane protein and *sec18* cells exhibited different phenotypes than the other *sec* mutants with respect to the endocytic pathway. *sec18* cells internalized α-factor more slowly than wild-type cells and accumulated α-factor in a membrane-bounded compartment not observed in *sec12* cells. These differences suggested that the phenotypes of the *sec18* mutant may be due to a direct function of the Sec18 protein in the endocytic pathway and not simply to an indirect effect of inhibiting ER → Golgi transport. To provide more evidence for this contention and to visualize the early endocytic compartment(s) that accumulated α-factor in *sec12* and *sec18* cells, we performed immunofluorescence microscopy with anti-Ste2p antiserum on wild-type and mutant cells preincubated for 5 min at 32°C. Figure 8a shows that in wild-type cells transport of the receptor upon α-factor binding occurred much as was seen at 30°C. *sec12* cells exhibited a different phenotype under these conditions. After exposure to α-factor, receptor was transported to a perivacuolar compartment in some cells; however, there was also intense staining of small more peripheral compartments that persisted even 30 min after α-factor addition. Note that the receptor staining in *sec12* cells resembles that seen in wild-type cells incubated at 15°C at early times after α-factor addition. The morphological data are consistent with results from endosome fractionation experiments indicating that membrane traffic through the early endosome is severely retarded in *sec12* at the nonpermissive temperature.

In this experiment, *sec18* exhibited a different phenotype than *sec12*. Receptor internalized into *sec18* cells at 32°C was seen in small vesicular structures distributed throughout the cytoplasm and never reached the perivacuolar late endosome. The endocytic phenotype of *sec18* suggests that it acts before the block imposed by inhibiting the secretory pathway. In addition, the role of Sec18p/NSF in promoting the fusion of transport vesicles with their target membrane is consistent with a role for Sec18p in the fusion of primary endocytic vesicles with, or to form, an early endosome. If this proposal is true, the endocytic phenotype of *sec18* should be epistatic to that of *sec12* even though in the secretory pathway the opposite is true (Kaiser and Schekman, 1990). To test this, we constructed a double mutant, *sec12sec18*, and visualized internalized receptor in the double mutant after addition of α-factor at 32°C. Figure 8b shows receptor

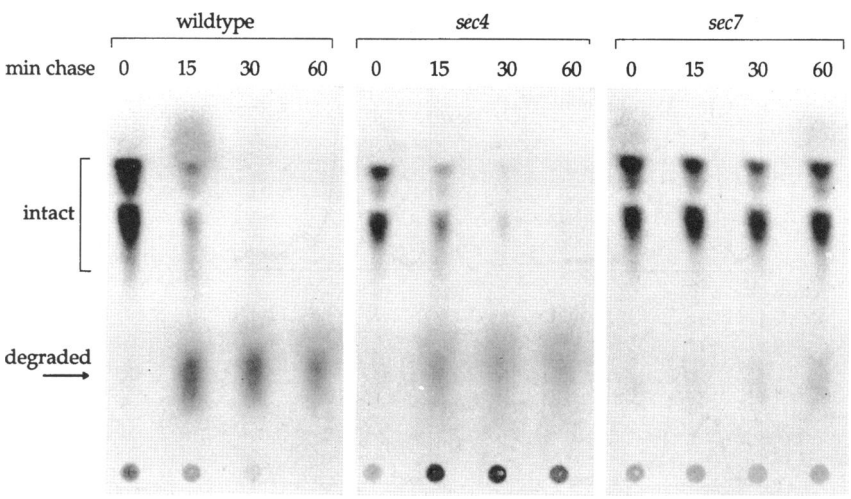

Figure 6. *sec* mutants that block early, but not late, steps of the secretory pathway are unable to efficiently degrade internalized α-factor. α-Factor degradation assays were performed on wild-type (RH448), *sec4* (RH1554), and *sec7* (RH1522) cells after a 15-min preincubation at 37°C. α-Factor was bound for 5 min and unbound peptide removed by centrifugation at 37°C. Cells were then resuspended in 37°C medium and aliquots were withdrawn at the indicated times. Cells were lysed and the α-factor extracted from lysates was analyzed by TLC to separate intact (bracket) and degraded (arrow) forms of the pheromone.

internalized in *sec12*, *sec18*, and *sec12sec18* cells at 32°C. The pattern of receptor staining in the double mutant resembles that of the *sec18* single mutant, not the *sec12* single mutant, demonstrating that the endocytic phenotype of *sec18* is epistatic to *sec12*.

BFA Inhibits Transport from the Yeast Early Endosome

The fungal metabolite BFA drastically disturbs the morphology of both secretory and endocytic organelles in mammalian cells. BFA prevents membrane transport between the ER and the Golgi yet does not seem to significantly disrupt recycling endocytic traffic. It is not clear how the drug affects endocytic traffic destined for lysosomes (Klausner *et al.*, 1992; Hunziker *et al.*, 1992).

Wild-type yeast are resistant to BFA. Mutations in the *ERG6* gene that is involved in synthesizing ergosterol render yeast sensitive to a number of drugs, including BFA. Treatment of mutant *erg6* cells with 75 μg/ml BFA leads to inhibition of membrane transport early in the secretory pathway (Graham *et al.*, 1993; Shah and Klausner, 1993; Vogel *et al.*, 1993). To test the effect of BFA on the yeast endocytic pathway, we assayed the ability of *erg6* cells to internalize and degrade α-factor in the presence of the drug. Figure 9a shows that internalization of α-factor proceeded with wild-type kinetics even at concentrations of up to 250 μg/ml BFA. In contrast, α-factor degradation is completely inhibited by BFA (Figure 9b).

To determine at which point the endocytic pathway is sensitive to BFA, we isolated and separated endosomes from *erg6* cells that had internalized α-factor in the presence of BFA. After a 10-min internalization, α-factor was detected equally in early and late endosomes in untreated cells but was found primarily in the early endosome of BFA-treated cells. Sixty minutes after internalization, α-factor was no longer observed in the endosomes isolated from wild-type cells. In the presence of BFA, α-factor remained and accumulated in the early endosome indicating that a complete block in transport had been imposed (Figure 9c).

DISCUSSION

In this article, we have shown that the α-factor receptor is delivered from the cell surface to the vacuole via at least two morphologically distinct compartments corresponding to the previously described early and late endosomes. Surprisingly, we found that transport of the receptor from the early to the late endosomal compartments depends on ongoing traffic in the early stages of the secretory pathway. However, at least one component required for early steps of the secretory pathway, Sec18p, is also directly required for endocytosis.

Early endosomes that mediate the transport of radiolabeled α-factor have been identified by subcellular fractionation (Singer and Riezman, 1990; Singer-Krüger *et al.*, 1993), and most likely correspond to the small peripheral elements that label with anti-receptor antibody at early time points in this study. Evidence that these peripheral structures are early endosomes comes from morphological and fractionation studies in the *sec12* and *sec18* mutants. In both cases, internalized α-factor accumulated at a restrictive temperature in organelles that cofractionated with early endosomes and, under similar conditions, the α-factor receptor was localized mainly at the periphery of the cells by immunofluorescence. As both α-factor and its receptor are internalized together, it is likely that they follow the same pathway to the vacuole. The early endosome may be heterogeneous in size or nature because the immunofluorescent labeling pattern seen in the *sec12* and *sec18* mutants was distinct.

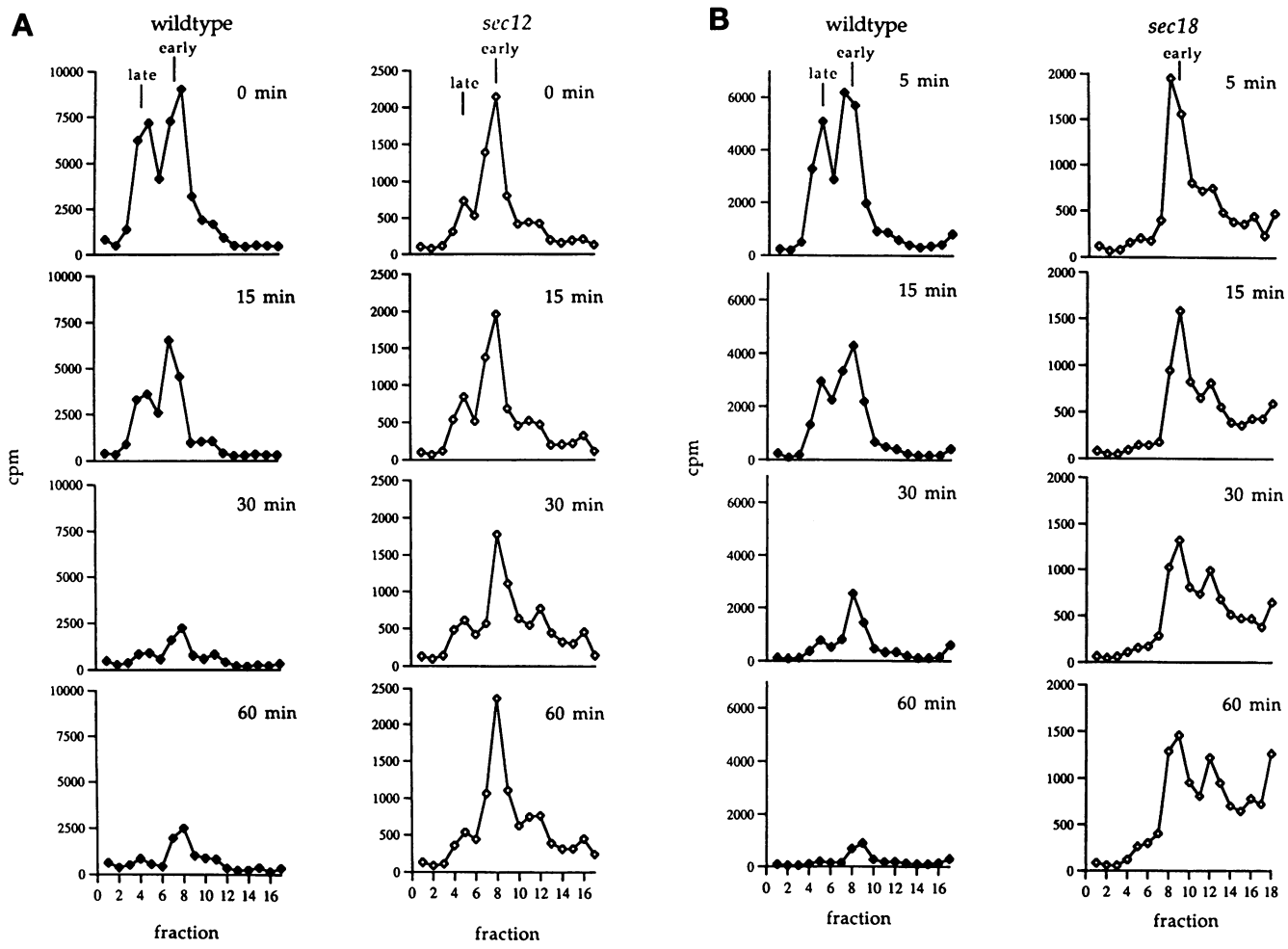

Figure 7. Blocking the early secretory pathway causes an immediate delay in transport from the early endosome. The P3 pellet fractions from cell lysates prepared at various times after α-factor internalization were resuspended in 37% Nycodenz, loaded under a Nycodenz density gradient, and centrifuged to equilibrium. Sixteen fractions were collected from each gradient and the amount of radioactivity associated with each, and with the gradient pellet (fraction 17 or 18), was determined by scintillation counting. The positions at which the early and late endosomes migrate in the gradients is indicated. The lower counts recovered in endosomes prepared from *sec* mutant cells was due to poorer lysis of these strains. (A) Wild-type (RH732) and *sec12* (RH2044) cells were preincubated for 5 min at 32°C, α-factor was bound and removed by centrifugation at 32°C, and cells were resuspend in 32°C YPUAD to begin chase of peptide through the endocytic pathway. The 0-min-chase time point corresponds to ≈10 min after the initiation of pheromone internalization. (B) Wild-type (RH732) and *sec18* (RH2043) cells were allowed to bind α-factor on ice, centrifuged at 4°C, and resuspended in 32°C YPUAD to initiate endocytosis of the peptide.

A recent study has demonstrated that the organelle that accumulates proteins en route to the vacuole in a subset of *vps* mutants is a functional prevacuolar intermediate (Piper *et al.*, 1995). Both endocytosed and newly synthesized vacuolar proteins pass through this compartment (Piper *et al.*, 1995). In this study we correlate the appearance of α-factor in the late endosome by subcellular fractionation with the accumulation of the α-factor receptor in a large perivacuolar compartment by immunofluorescence. Our results strongly suggest that this late endosome is the previously described prevacuolar compartment.

The late endosomal compartment was visualized in more detail by immunogold labeling and its morphology is similar to what has been described for the late endosome in animal cells (Griffiths *et al.*, 1988; McDowall *et al.*, 1989). In cross-section it appears to be multivesicular in nature with internal membranes. Also similar to the situation in animal cells, the late endosome is localized more toward the interior of the cell than early endosomes, but in yeast the compartment is near the vacuole rather than juxtanuclear.

Endocytic Transport Is Obligatorily Coupled to the Early Secretory Pathway

We have found that *sec* mutations that block ER → Golgi and intraGolgi transport inhibit endocytic trans-

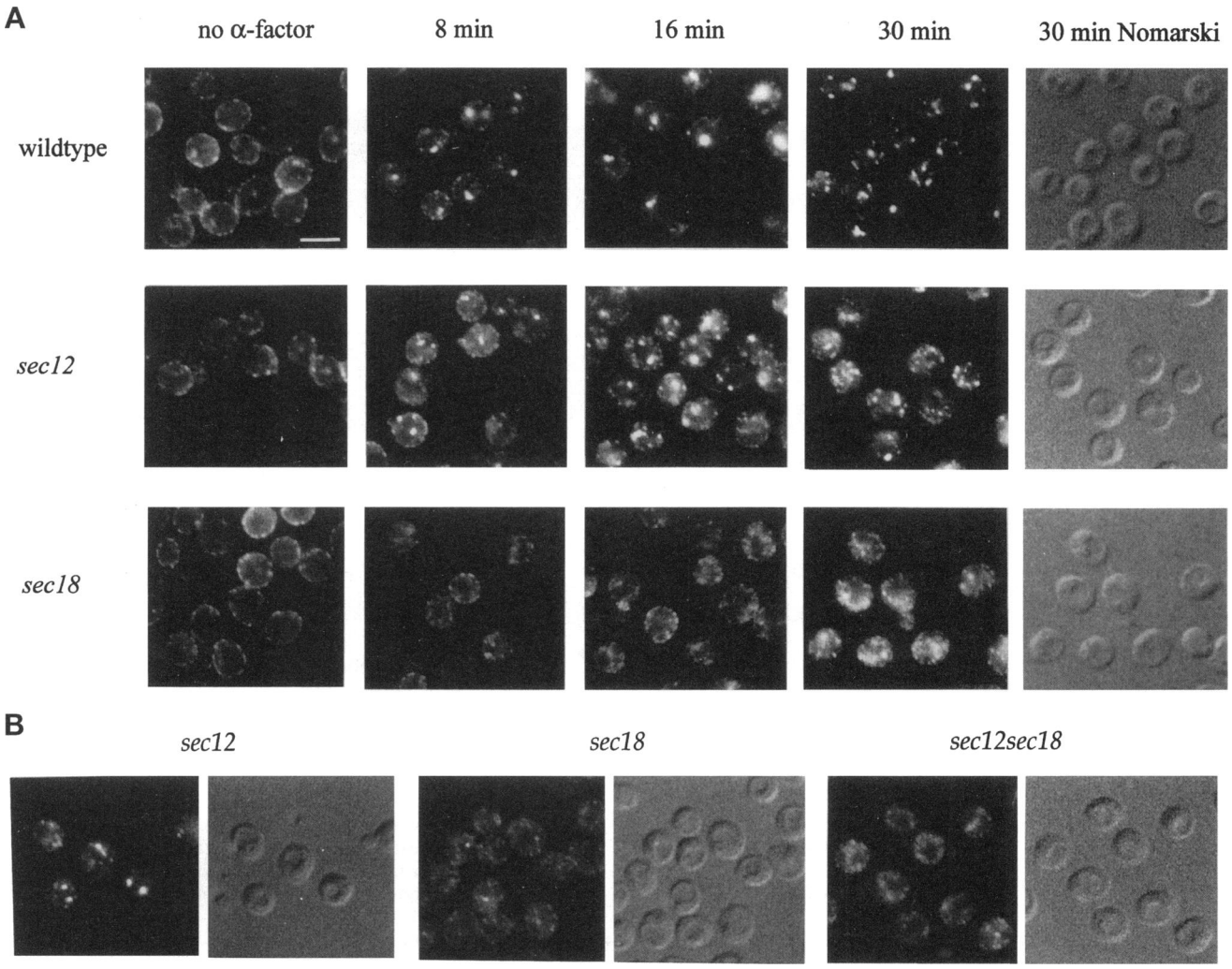

Figure 8. In the absence of active Sec18p/NSF, α-factor receptor accumulates in small vesicular structures. (A) Immunofluorescent localization of Ste2p in wild-type (RH448), *sec12* (RH1491), and *sec18* (RH1737) cells before the addition of α-factor (no α-factor) and at 8, 16, and 30 min after exposure cells to α-factor. Cells were preincubated at 32°C and incubation was continued at this temperature after pheromone addition. (B) Localization of Ste2p in *sec12* (RH1491), *sec18* (RH1737), and *sec12sec18* (RH2465) strains at 16 min after addition of α-factor to the cells at 32°C.

port of α-factor and its receptor from the early endosome, whereas mutations that block Golgi → plasma membrane transport do not. In this study we found that all ER → Golgi *sec* mutations inhibited α-factor transport through the endocytic pathway to some degree. This is in contrast to results obtained when the fluid-phase marker lucifer yellow was used to analyze endocytosis in *sec* mutants (Riezman, 1985). *sec14*, *sec20*, and *sec21* were found to accumulate lucifer yellow in the vacuole although other ER → Golgi *sec* mutants did not. We believe that this discrepancy simply reflects differences in the two assays. The assays for α-factor internalization and transport are significantly more sensitive and quantitative than the lucifer yellow assay. The mutants that were interpreted to endocytose normally because they accumulated lucifer yellow in the vacuole are somewhat leaky and are less defective in α-factor transport than the other ER → Golgi and intraGolgi mutants.

Furthermore, in the previous work the late *sec* mutants *sec1*, *sec2*, and *sec5* were defective in accumulation of lucifer yellow in the vacuole after a 1-h incubation at the nonpermissive temperature. In this article, we report that α-factor is transported at wild-type rates in *sec5* at 37°C. The recent experiments were performed with shorter preincubations that are sufficient to completely inhibit the secretory pathway. Therefore, the defect in lucifer yellow transport observed previously is an indirect effect due to the ex-

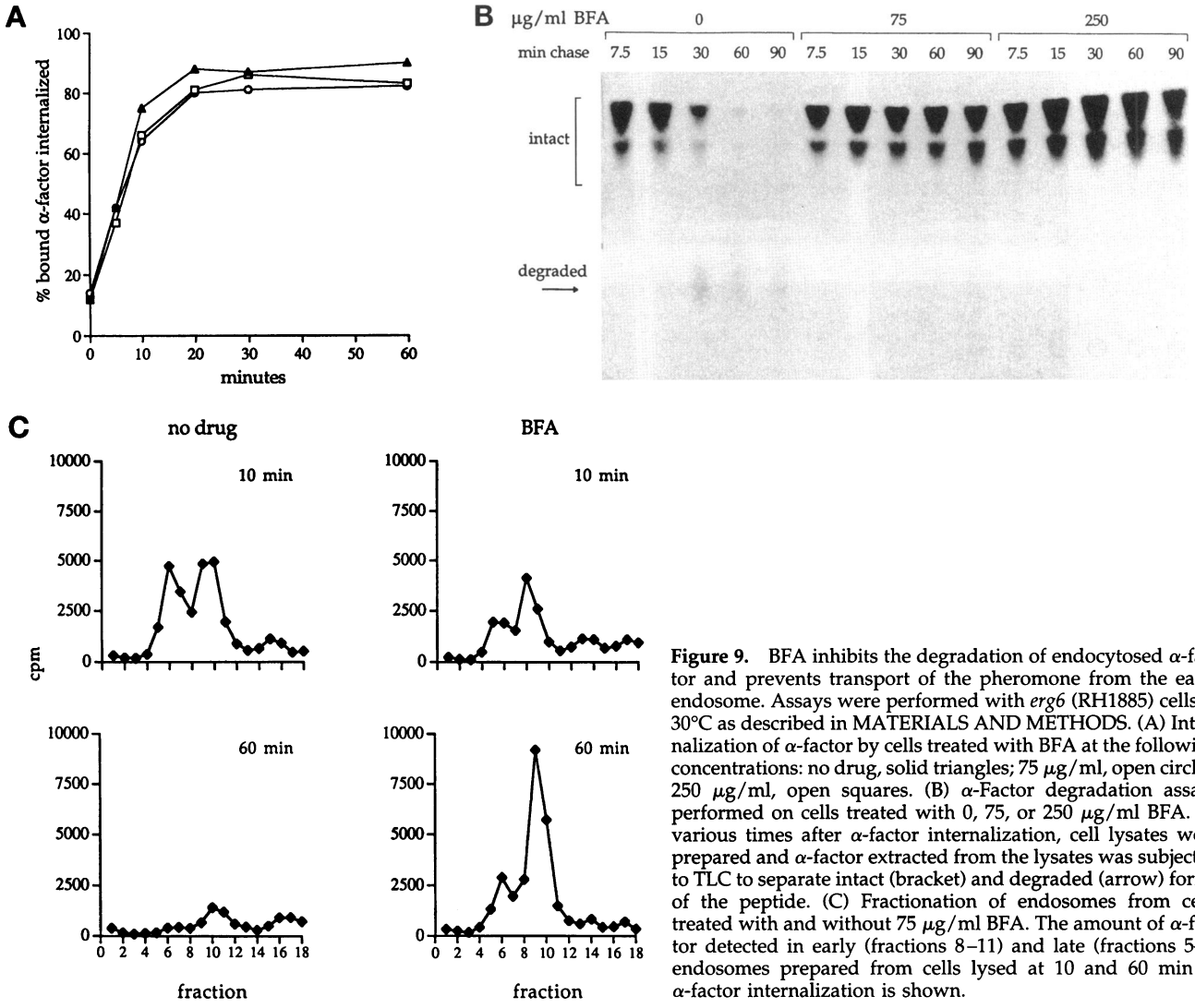

Figure 9. BFA inhibits the degradation of endocytosed α-factor and prevents transport of the pheromone from the early endosome. Assays were performed with *erg6* (RH1885) cells at 30°C as described in MATERIALS AND METHODS. (A) Internalization of α-factor by cells treated with BFA at the following concentrations: no drug, solid triangles; 75 μg/ml, open circles; 250 μg/ml, open squares. (B) α-Factor degradation assays performed on cells treated with 0, 75, or 250 μg/ml BFA. At various times after α-factor internalization, cell lysates were prepared and α-factor extracted from the lysates was subjected to TLC to separate intact (bracket) and degraded (arrow) forms of the peptide. (C) Fractionation of endosomes from cells treated with and without 75 μg/ml BFA. The amount of α-factor detected in early (fractions 8–11) and late (fractions 5–7) endosomes prepared from cells lysed at 10 and 60 min of α-factor internalization is shown.

tended incubation of mutant cells at the nonpermissive temperature.

We have demonstrated that α-factor and its receptor accumulate in the early endosome in ER → Golgi *sec* mutants at the nonpermissive temperature. It is unlikely that this observation reflects a direct requirement for most Sec proteins at the endosome as the localization of some of the proteins (e.g., Sec12p) is restricted to the organelles of the early secretory pathway. The need for an active biosynthetic pathway suggests that some molecule(s) must be continuously delivered into the endosomal system from the secretory pathway. Because delivery of this factor does not require the late secretory pathway, it may be transferred directly from the Golgi to the early endosome. This pathway has not been observed in yeast, but evidence for such a route exists in mammalian cells (Sariola *et al.*, 1995). Alternatively, the component could travel from the Golgi to the late endosome and function in early to late endosomal traffic at the downstream location.

Inhibiting protein synthesis does not block early to late endosome traffic, suggesting that the factor delivered through the secretory pathway is not a newly synthesized protein. It could be a protein that repeatedly cycles from ER to Golgi to the early endosome and then back to the ER. We consider this unlikely because, though traffic from endosome to the ER has been demonstrated for toxins (Sandvig *et al.*, 1994), proteins have not yet been observed to travel a full ER → endosome → ER cycle. It is more likely that either membrane components in bulk or a specific newly synthesized lipid must be delivered from the ER → Golgi → early endosome. At the endosome, a lipid could be irreversibly modified, consumed, or transported through the endocytic pathway to the vacuole

where it would be destroyed. Lipids, or proteins that modify them, have been shown to be important for several membrane trafficking steps in yeast, including vacuole biogenesis (Schu *et al.*, 1993), endocytosis (Munn and Riezman, 1994), ER → Golgi transport of glycosylphosphatidylinositol-anchored proteins (Horvath *et al.*, 1994), and exit from the Golgi (Cleves *et al.*, 1991). A phosphatidylinositide may be a lipid required at the early endosome as the PI-3 kinase, Vps34p, has been shown to be required for the efficient transport of internalized α-factor to the vacuole (Munn and Riezman, 1994).

The requirement for continuous delivery of a molecule from the Golgi to endosomes to promote endocytic traffic ensures a tight coupling or balance between the secretory and endocytic pathways. This could be important in a cell such as yeast that expands its plasma membrane continuously during rapid growth and changes its growth rate depending on nutrient availability and temperature.

Molecular Mechanisms Involved in the Yeast Endocytic Pathway

Sec18p/NSF is required at multiple steps in the secretory pathway in both yeast and mammalian cells (Graham and Emr, 1991; Rothman and Orci, 1992) and is required for the fusion of early endosomes with each other in vitro (Diaz *et al.*, 1989). We have now shown that Sec18p is required in vivo for the forward progression of molecules from the plasma membrane to the vacuole in yeast. α-Factor internalized in a *sec18* strain at the nonpermissive temperature is found in an endosomal compartment of the same density as the early endosome. Because ER → Golgi transport is inhibited in the *sec18* mutant and because we have shown that an active secretory pathway is necessary for efficient membrane transport from the early endosome, it could be that the requirement of Sec18p in the endocytic pathway is merely due to its activity in ER → Golgi transport. This is probably not the case because the *sec18* mutant exhibits a different endocytic phenotype than the other ER → Golgi *sec* mutants and this phenotype is epistatic to the block imposed by inhibiting the secretory pathway. In *sec18* cells incubated at the nonpermissive temperature, internalized α-factor receptor accumulates in many small peripheral vesicles, a staining pattern distinctly different from that observed in *sec12* cells under the same conditions. Furthermore, in a *sec12sec18* double mutant receptor accumulates in the same pattern as that observed for the *sec18* single mutant, demonstrating that in the endocytic pathway Sec18p acts before the step at which input from the secretory pathway is required.

The role of Sec18p/NSF in secretion is to promote the fusion of transport vesicles with their target membranes, a process that occurs between two different types of membranes and has been referred to as heterotypic fusion. Some homotypic fusion events that occur between membranes of secretory organelles have been shown to be independent of Sec18p/NSF and to require a related protein known as Cdc48p/p97 (Acharya *et al.*, 1995; Latterich *et al.*, 1995; Rabouille *et al.*, 1995). However, Sec18p has been shown to be required for homotypic fusion in the endocytic pathway in cell-free systems in animal cells (Diaz *et al.*, 1989, Rodriguez *et al.*, 1994). In addition, Sec18p/NSF is required to mediate the homotypic fusion of vacuolar membrane that occurs during the in vitro reconstitution of vacuole inheritance in yeast (Mayer *et al.*, 1996). Our results are consistent with a function for Sec18p early in the endocytic pathway after internalization. Sec18p may promote the homotypic fusion of primary endocytic vesicles with each other to form a more mature early endosome or may be involved in the heterotypic fusion of primary endocytic vesicles with a preexisting early endosome. Another member of the Sec18/Ccd48/Pas1 family of ATPases may also function in the endocytic pathway. The *END13* gene that is required for efficient postinternalization endocytic membrane transport encodes such an ATPase (Stevenson and Riezman, unpublished data; GenBank accession no. U25843).

Treatment of mammalian cells with BFA drastically alters the morphology of their endocytic organelles. Internalization and recycling of receptors appear to continue in the presence of BFA. Other endocytic traffic events are disrupted by the drug, including the delivery of fluid-phase markers to the lysosome (Lippincott-Schwartz *et al.*, 1991) and the transcytosis of IgA from the basolateral to the apical surfaces of MDCK cells (Hunziker *et al.*, 1991). Treatment of sensitive yeast with BFA causes a complete block in transport from the early endosome although there is no effect on the earlier internalization step. Immunofluorescence experiments indicate that BFA probably also alters the morphology of yeast endosomes (our unpublished data). BFA inhibits traffic through the early secretory pathway and this may be the explanation for its dramatic effect on endocytosis. It is likely though that BFA inhibits endocytic traffic directly. The effect of BFA on endocytosis is immediate and requires no preincubation of cells with the drug. In addition, BFA causes an absolute block in transport, no α-factor is degraded in the presence of BFA and peptide transport through the early endosome was prevented completely. This is in contrast to the effect seen by inhibiting the biosynthetic pathway in most of the *sec* mutants, in which traffic through the endosome is severely retarded but not completely inhibited.

BFA blocks the binding of cytoplasmic coat proteins that mediate vesicle budding to organelles. Coat complexes composed of COPI proteins have recently been shown to assemble onto endosomes in vitro in a BFA-

sensitive manner, suggesting that these proteins participate in endosomal transport (Whitney *et al.*, 1995). In yeast, however, COPI proteins encoded by the *RET1* (α-COP) and *SEC27* (β'-COP) genes do not seem to be required for forward endocytic transport as α-factor degradation occurs normally in cells carrying mutations in these genes (Table 2). It is possible that another coat complex mediates endocytic transport.

ACKNOWLEDGMENTS

Strains used in this study were generously provided by Randy Schekman, Tom Stevens, and Rick Gaber. BFA and 9E10 c-myc antiserum were gifts from Sandoz Pharmaceuticals (Basel, Switzerland). We thank Markus Dürrenberger for advice and help with confocal microscopy. We are grateful to Nicolas Stern for media and to Thomas Aust for cheerfully purifying lots of lyticase. This manuscript was improved by the critical comments of Maribel Geli, Stephan Schröder, and Andreas Wesp. L.H. was supported by a postdoctoral fellowship from the American Cancer Society and M.P. was the recipient of European Molecular Biology Organization and Human Science Program Organization postdoctoral fellowships. This work was funded by the Swiss National Science Foundation and the Canton Basel Stadt.

REFERENCES

Acharya, U., Jacobs, R., Peters, J.-M., Watson, N., Farquhar, M.G., and Malhotra, V. (1995). The formation of Golgi stacks from vesiculated Golgi membranes requires two distinct fusion events. Cell *82*, 895–905.

Aniento, F., Gu, F., Parton, R.G., and Gruenberg, J. (1996). An endosomal β-COP is involved in the pH-dependent formation of transport vesicles destined for late endosomes. J. Cell Biol. *133*, 29–41.

Chvatchko, Y., Howald, I., and Riezman, H. (1986). Two yeast mutants defective in endocytosis are defective in pheromone response. Cell *46*, 355–364.

Cleves, A.E., McGee, T.P., Whitters, E.A., Campion, K.M., Aitken, J.R., Dowhan, W., Goebl, M., and Bankaitis, V.A. (1991). Mutations in the CDP-choline pathway for phospholipid biosynthesis bypass the requirement for an essential phospholipid transfer protein. Cell *64*, 789–800.

Colombo, M.I., Mayorga, L.S., Casey, P.J., and Stahl, P.D. (1992). Evidence of a role for heterotrimeric GTP-binding proteins in endosome fusion. Science *255*, 1695–1697.

Davis, N.G., Horecka, J.L., and Sprague, G.F. (1993). Cis- and trans-acting functions required for endocytosis of the yeast pheromone receptors. J. Cell Biol. *122*, 53–65.

De Camilli, P., Emr, S.D., McPherson, P.S., and Novick, P. (1996). Phosphoinositides as regulators in membrane traffic. Science *271*, 1533–1539.

Diaz, R., Mayorga, L.S., Weidman, P.J., Rothman, J.E., and Stahl, P.D. (1989). Vesicle fusion following receptor-mediated endocytosis requires a protein active in Golgi transport. Nature *339*, 398–400.

D'Souza-Schorey, C., Li, G., Colombo, M.I., and Stahl, P.D. (1995). A regulatory role for ARF6 in receptor-mediated endocytosis. Science *267*, 1175–1178.

Dulic, V., Egerton, M., Elguindi, I., Raths, S., Singer, B., and Riezman, H. (1991). Yeast endocytosis assays. Methods Enzymol. *194*, 697–710.

Evan, G.I., Lewis, G.K., Ramsay, G., and Bishop, J.M. (1985). Isolation of monoclonal antibodies specific for human c-*myc* proto-oncogene product. Mol. Cell. Biol. *5*, 3610–3616.

Feng, Y., Press, B., and Wandinger-Ness, A. (1995). Rab7: an important regulator of late endocytic membrane traffic. J. Cell Biol. *131*, 1435–1452.

Gammie, A.E., Kurihara, L.J., Vallee, R.B., and Rose, M.D. (1995). *DNM1*, a dynamin-related gene, participates in endosomal trafficking in yeast. J. Cell Biol. *130*, 553–566.

Graham, T.R., and Emr, S.D. (1991). Compartmental organization of Golgi-specific protein modification and vacuolar protein sorting events defined in a yeast *sec18* (NSF) mutant. J. Cell Biol. *114*, 207–218.

Graham, T.R., Scott, P.A., and Emr, S.D. (1993). Brefeldin A reversibly blocks early but not late protein transport steps in the yeast secretory pathway. EMBO J. *12*, 869–877.

Griffiths, G., Hoflack, B., Simons, K., Mellman, I., and Kornfeld, S. (1988). The mannose 6-phosphate receptor and the biogenesis of lysosomes. Cell *52*, 329–341.

Gruenberg, J., and Emans, N. (1993). Annexins in membrane traffic. Trends Cell Biol. *3*, 224–227.

Gruenberg, J., and Maxfield, F.R. (1995). Membrane transport in the endocytic pathway. Curr. Opin. Cell Biol. *7*, 552–563.

Helenius, A., Mellman, I., Wall, D., and Hubbard, A. (1983). Endosomes. Trends Biochem. Sci. *8*, 245–250.

Hicke, L., and Riezman, H. (1996). Ubiquitination of a yeast plasma membrane receptor signals its ligand-stimulated endocytosis. Cell *84*, 277–287.

Horazdovsky, B.F., Busch, G.R., and Emr, S.D. (1994). *VPS21* encodes a rab5-like GTP-binding protein that is required for the sorting of yeast vacuolar proteins. EMBO J. *13*, 1297–1309.

Horvath, A., Sütterlin, C., Manning-Krieg, U., Movva, N.R., and Riezman, H. (1994). Ceramide synthesis enhances transport of GPI-anchored proteins to the Golgi apparatus in yeast. EMBO J. *13*, 3687–3695.

Hunziker, W., Whitney, J.A., and Mellman, I. (1991). Selective inhibition of transcytosis by brefeldin A in MDCK cells. Cell *67*, 617–627.

Hunziker, W., Whitney, J.A., and Mellman, I. (1992). Brefeldin A and the endocytic pathway. FEBS Lett. *307*, 93–96.

Kaiser, C.A., and Schekman, R. (1990). Distinct sets of *SEC* genes govern transport vesicle formation and fusion early in the secretory pathway. Cell *61*, 723–733.

Klausner, R.D., Donaldson, J.G., and Lippincott-Schwartz, J. (1992). Brefeldin A: insights into the control of membrane traffic and organelle structure. J. Cell Biol. *116*, 1071–1080.

Latterich, M., Fröhlich, K.-U., and Schekman, R. (1995). Membrane fusion and the cell cycle: Cdc48p participates in the fusion of ER membranes. Cell *82*, 885–893.

Lippincott-Schwartz, J., Yuan, L., Tipper, C., Amherdt, M., Orci, L., and Klausner, R.D. (1991). Brefeldin A's effects on endosomes, lysosomes, and the TGN suggest a general mechanism for regulating organelle structure and membrane traffic. Cell *67*, 601–616.

Mayer, A., Wickner, W., and Haas, A. (1996). Sec18p(NSF)-driven release of Sec17p(α-SNAP) can precede docking and fusion of yeast vacuoles. Cell *85*, 83–94.

McDowall, A., Gruenberg, J., Römisch, K., and Griffiths, G. (1989). The structure of organelles of the endocytic pathway in hydrated cryosections of cultured cells. Eur. J. Cell Biol. *49*, 281–294.

Munn, A.L., and Riezman, H. (1994). Endocytosis is required for the growth of vacuolar H^+-ATPase-defective yeast: identification of six new *END* genes. J. Cell Biol. *127*, 373–386.

Munn, A.L., Stevenson, B.J., Geli, M.I., and Riezman, H. (1995). end5, *end6*, and *end7*: mutations that cause actin delocalization and block the internalization step of endocytosis in *Saccharomyces cerevisiae*. Mol. Biol. Cell *6*, 1721–1742.

Nakano, A., Brada, D., and Schekman, R. (1988). A membrane glycoprotein, Sec12p, required for protein transport from the endoplasmic reticulum to the Golgi apparatus in yeast. J. Cell Biol. *107*, 851–863.

Nilsson, T., Pypaert, M., Hoe, M.H., Slusarewicz, P., Berger, E.G., and Warren, G. (1993). Overlapping distribution of two glycosyltransferases in the Golgi apparatus of HeLa cells. J. Cell Biol. *120*, 5–13.

Nishikawa, S.-I., and Nakano, A. (1993). Identification of a gene required for membrane protein retention in the early secretory pathway. Proc. Natl. Acad. Sci. USA *90*, 8179–8183.

Peters, P.J., Hsu, V.W., Ooi, C.E., Finazzi, D., Teal, S.B., Oorschot, V., Donaldson, J.G., and Klausner, R.D. (1995). Overexpression of wild-type and mutant ARF1 and ARF6: distinct perturbations of non-overlapping membrane compartments. J. Cell Biol. *128*, 1003–1017.

Piper, R.C., Cooper, A.A., Yang, H., and Stevens, T.H. (1995). *VPS27* controls vacuolar and endocytic traffic through a prevacuolar compartment in *Saccharomyces cerevisiae*. J. Cell Biol. *131*, 603–617.

Rabouille, C., Levine, T.P., Peters, J.-M., and Warren, G. (1995). An NSF-like ATPase, p97, and NSF mediate cisternal regrowth from mitotic Golgi fragments. Cell *82*, 905–914.

Raths, S., Rohrer, J., Crausaz, F., and Riezman, H. (1993). *end3* and *end4*: two mutants defective in receptor-mediated and fluid-phase endocytosis in *Saccharomyces cerevisiae*. J. Cell Biol. *120*, 55–65.

Raymond, C.K., Howald-Stevenson, I., Vaters, C.A., and Stevens, T.H. (1992). Morphological classification of the yeast vacuolar protein sorting mutants: evidence for a prevacuolar compartment in class E vps mutants. Mol. Biol. Cell *3*, 1389–1402.

Riezman, H. (1985). Endocytosis in yeast: several of the yeast secretory mutants are defective in endocytosis. Cell *40*, 1001–1009.

Riezman, H. (1993). Yeast endocytosis. Trends Cell Biol. *3*, 273–277.

Rodriguez, L., Stirling, C.J., and Woodman, P.G. (1994). Multiple N-ethylmaleimide-sensitive components are required for endosomal vesicle fusion. Mol. Biol. Cell *5*, 773–783.

Rohrer, J., Bénédetti, H., Zanolari, B., and Riezman, H. (1993). Identification of a novel sequence mediating regulated endocytosis of the G-protein-coupled α-pheromone receptor in yeast. Mol. Biol. Cell *4*, 511–521.

Rothman, J.E., and Orci, L. (1992). Molecular dissection of the secretory pathway. Nature *355*, 409–415.

Sandvig, K., Ryd, M., Garred, O., Schweda, E., Holm, P.K., and van Deurs, B. (1994). Retrograde transport from the Golgi complex to the ER of both Shiga toxin and the nontoxic Shiga B-fragment is regulated by butyric acid and cAMP. J. Cell Biol. *126*, 53–64.

Sariola, M., Saraste, J., and Kuismanen, E. (1995). Communication of post-Golgi elements with early endocytic pathway: regulation of endoproteolytic cleavage of Semliki Forest virus p62 precursor. J. Cell Sci. *108*, 2465–2475.

Schimmöller, F., and Riezman, H. (1993). Involvement of Ypt7p, a small GTPase, in traffic from late endosome to the vacuole in yeast. J. Cell Sci. *106*, 823–830.

Schu, P.V., Takegawa, K., Fry, M.J., Stack, J.H., Waterfield, M.D., and Emr, S.D. (1993). Phosphatidylinositol 3-kinase encoded by yeast VPS34 gene essential for protein sorting. Science *260*, 88–91.

Shah, N., and Klausner, R.D. (1993). Brefeldin A reversibly inhibits secretion in *Saccharomyces cerevisiae*. J. Biol. Chem. *268*, 5345–5348.

Shen, S.-H., Chretien, P.L.B., and Slilaty, S.N. (1991). Primary sequence of the glucanase gene from *Oerskovia xanthineolytica*. J. Biol. Chem. *266*, 1058–1063.

Simons, K., and Zerial, M. (1993). Rab proteins and the road maps for intracellular transport. Neuron *11*, 789–799.

Singer, B., and Riezman, H. (1990). Detection of an intermediate compartment involved in transport of α-factor from the plasma membrane to the vacuole in yeast. J. Cell Biol. *110*, 1911–1922.

Singer-Krüger, B., Frank, R., Crausaz, F., and Riezman, H. (1993). Partial purification and characterization of early and late endosomes from yeast. J. Biol. Chem. *268*, 14376–14386.

Singer-Krüger, B., Stenmark, H., Duesterhoeft, A., Philippsen, P., Yoo, J.-S., Gallwitz, D., and Zerial, M. (1994). Role of three rab5-like GTPases, Ypt51p, Ypt52p, and Ypt53p, in the endocytic and vacuolar protein sorting pathways of yeast. J. Cell Biol. *125*, 283–298.

Vogel, J.P., Lee, J.N., Kirsch, D.R., Rose, M.D., and Sztul, E.S. (1993). Brefeldin A causes a defect in secretion in *Saccharomyces cerevisiae*. J. Biol. Chem. *268*, 3040–3043.

Whitney, J.A., Gomez, M., Sheff, D., Kreis, T.E., and Mellman, I. (1995). Cytoplasmic coat proteins involved in endosome function. Cell *83*, 703–713.

Wichmann, H., Hengst, L., and Gallwitz, D. (1992). Endocytosis in yeast: evidence for the involvement of a small GTP-binding protein (Ypt7p). Cell *71*, 1131–1142.

Zanolari, B., and Riezman, H. (1991). Quantitation of α-factor internalization and response during the *Saccharomyces cerevisiae* cell cycle. Mol. Cell. Biol. *11*, 5251–5258.

Zanolari, B., Raths, S., Singer-Krüger, B., and Riezman, H. (1992). Yeast pheromone receptor endocytosis and hyperphosphorylation are independent of G-protein-mediated signal transduction. Cell *71*, 755–763.